BIOCHEMISTRY
including biophysical chemistry & molecular biology

Article

pubs.acs.org/biochemistry

Formation of G-Quadruplexes in Poly-G Sequences: Structure of a Propeller-Type Parallel-Stranded G-Quadruplex Formed by a G_{15} Stretch

Anjali Sengar, Brahim Heddi, and Anh Tuân Phan*

School of Physical and Mathematical Sciences, Nanyang Technological University, Singapore 637371, Singapore

Supporting Information

ABSTRACT: Poly-G sequences are found in different genomes including human and have the potential to form higher-order structures with various applications. Previously, long poly-G sequences were thought to lead to multiple possible ways of G-quadruplex folding, rendering their structural characterization challenging. Here we investigate the structure of G-quadruplexes formed by poly-G sequences d(TTG_nT), where n = 12 to 19. Our data show the presence of multiple and/or higher-order G-quadruplex structures in most sequences. Strikingly, NMR spectra of the $TTG_{15}T$ sequence containing a stretch of 15 continuous guanines are exceptionally well-resolved and indicate the formation of a well-defined G-quadruplex structure. The NMR solution structure of this sequence revealed a propeller-type parallel-stranded G-quadruplex containing three G-tetrad layers and three single-guanine propeller loops. The same structure can potentially form anywhere along a long G_n stretch, making it unique for molecular recognition by other cellular molecules.

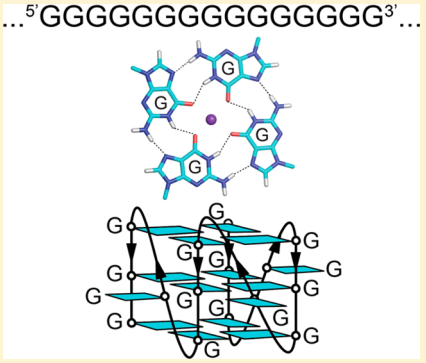

Guanines (G) have a high potential for self-recognition and self-assembly. Four guanines can be held together by Hoogsteen hydrogen bonds in a planar G-tetrad.[1] In a G-rich nucleic acid sequence, multiple G-tetrads can form and stack on top of each other, resulting in a four-stranded structure called a G-quadruplex, further stabilized by cations.[2−4] Potential G-quadruplex-forming sequences are abundant in the genomes of different species.[5−8] Bioinformatics analysis revealed over 350 000 putative G-quadruplex-forming sequences containing at least four short tracts of three or more continuous guanines in the human genome[5,6] including important regions such as telomeres,[9] promoters,[10] immunoglobulin switch regions, and recombination hot spots.[11] Increasing evidence for the existence and functions of G-quadruplexes *in vivo* have been reported.[12−15] In particular, G-quadruplexes in the telomeres and oncogenic promoters are considered attractive anticancer drug targets.[16,17]

It has been found that long poly-G tracts are abundantly distributed in the genome of *C. elegans* and *C. briggsae*.[18] In *C. elegans*, there are approximately 400 poly-G regions of various lengths (∼10−30 nucleotides) in different chromosomes.[19] G-repeats have been shown to play an important role in phase variable gene expression in pathogenic bacteria *Helicobacter pylori*.[20,21] Poly-G regions are also found in the human genome. For instance, in chromosome 2 there is a 427-nt region, where only 24 out of 427 nucleotides are non-guanines.[22]

From a molecular engineering perspective, G-quadruplex-forming sequences can be important as therapeutic agents, possessing anticancer, anti-HIV, or anticoagulant properties.[23] In addition, G-quadruplex scaffolds were used for nano- and microparticle assemblies[24,25] or as electronic switches[26] and drug carriers.[27,28] In particular, microcapsules containing G-quadruplexes formed by G_{15}-mer oligonucleotides have been demonstrated as promising therapeutic carriers.[29] Poly-G sequences also have the potential to form higher-order structures such as nanowires.[30] G-quadruplex-based nanowires have high stiffness and rigidity that are generally considered crucial elements for their applicability in nanoelectronics.[31,32]

Structures of many G-quadruplexes have been determined by NMR and X-ray crystallography, illustrating a rich diversity in the folding topology depending on the sequence.[3,4,17,33−42] To date, structural studies of G-quadruplexes have been mostly limited to sequences containing short tracts of continuous guanines (which form the columns supporting the G-tetrad core) separated by non-guanine residues (which form loops). NMR and X-ray crystallographic structures of G-quadruplexes formed by a tract of 3 or 4 continuous guanines (e.g., TG_3T and TG_4T) revealed tetrameric parallel-stranded G-quadruplexes, where all guanines adopt an *anti* conformation.[43] Despite the general belief that long poly-G sequences would form tetrameric G-quadruplexes, recent mass spectrometry experiments showed that these sequences folded into G-quadruplexes of lower stoichiometry,[44] in accordance with an early model of a monomeric fold-back G-quadruplex.[45] However, high-resolution structures of G-quadruplexes formed by long G_n tracts have not been studied.

Received: August 8, 2014
Revised: October 31, 2014
Published: November 6, 2014

dx.doi.org/10.1021/bi500990v | *Biochemistry* 2014, 53, 7718−7723

In this work, using Nuclear Magnetic Resonance (NMR) and Circular Dichroism (CD) spectroscopy, we investigate the structure of G-quadruplexes formed in DNA poly-G sequences d(TTG$_n$T), where n ranges from 12 to 19. Two thymines at the 5′-end and one at the 3′-end were added to help prevent the stacking and aggregation of G-quadruplex blocks, hence, facilitating a NMR structural study.[46] Unexpectedly, we discovered that the d(TTG$_{15}$T) sequence displayed exceptionally well-resolved NMR spectra and showed that it formed a single parallel-stranded G-quadruplex containing three G-tetrad layers and three single-guanine propeller loops. Such a unique G-quadruplex motif can be biologically relevant, as it can potentially be formed by a fragment of 15 continuous guanines anywhere along a poly-G sequence.

METHODS

Sample Preparation. DNA oligonucleotides were chemically synthesized on an ABI 394 DNA synthesizer using products from Glen Research and Cambridge Isotope Laboratories and then purified following the protocol from Glen Research. The samples (concentration, 0.02−0.20 mM) were dialyzed successively against water, 2 mM KCl, and water again. DNA oligonucleotides were frozen, lyophilized, and dissolved in buffer containing 2 mM KCl and 10 mM Tris−HCl buffer (pH 7). The DNA concentration was expressed in strand molarity using a nearest neighbor approximation for the 260-nm molar extinction coefficient of the unfolded species.

Gel Electrophoresis. The molecular size of oligonucleotides was visualized by non-denaturing gel electrophoresis. Oligonucleotides were prepared in 10 mM Tris-HCl buffer (pH 7), supplemented with 2 mM KCl. The samples were loaded on a 20% polyacrylamide gel, supplemented with 2 mM KCl; 10% sucrose was added just before loading. The gel was viewed by UV shadowing.

UV Spectroscopy. The stability of G-quadruplexes was measured in UV melting experiments conducted on a JASCO V-650 spectrophotometer. Experiments were performed with 1-cm path length quartz cuvettes. The absorbance at 295 nm was recorded as a function of temperature ranging from 20 to 90 °C. Heating and cooling were done at a rate of 0.2 °C/min. The DNA concentration ranged from 4 to 6 μM. The solution contained 5 mM KCl and 10 mM Tris-HCl buffer (pH 7). To calculate the DNA folded fraction, all UV melting curves are manually fitted for two-state folding where two baselines are drawn at low and high temperatures corresponding to completely folded and unfolded states. For each sequence the melting temperature (T_m) for unfolding is presented. The difference in the T_m values from folding and unfolding was less than 1 °C.

CD Spectroscopy. CD spectra were recorded on a JASCO-815 spectropolarimeter using a 1-cm path length quartz cuvette in a reaction volume of 500 μL at 20 °C. Scans from 220 to 320 nm were performed with a rate of 200 nm/min, 1-nm pitch, and 1-nm bandwidth. The DNA concentration ranged from 4 to 6 μM. For each experiment, an average of three scans was taken, the spectrum of the buffer with 5 mM KCl and 10 mM Tris-HCl was subtracted, and data were zero-corrected at 320 nm.

NMR Spectroscopy. NMR experiments were performed on Bruker Advance spectrometers operating at 600 or 700 MHz for ^{1}H at 25 °C. The DNA concentration for NMR experiments was typically 0.2−2.0 mM. Spectral assignments of ***G15*** were obtained by comparison with the spectra of ***T95-2T*** and completed by using NOESY and TOCSY spectra. Thymine resonances were identified by the through-bond H6-CH$_3$ correlations from TOCSY spectra.[47] The folding topologies and more detailed structural information on G-quadruplexes were obtained from NOESY spectra.

Structure Calculation. The NMR structure of the ***G15*** G-quadruplex was calculated based on distance-restrained molecular dynamics refinement following distance geometry simulated annealing using the program XPLOR-NIH.[48] Detailed procedures for structure calculation are described previously.[46] Interproton distances were deduced from NOESY spectra. Structures were displayed using the program PyMOL.[49]

Data Deposition. The coordinates for the ***G15*** G-quadruplex have been deposited in the Protein Data Bank (accession code 2MB2).

RESULTS AND DISCUSSION

G-Quadruplexes Formed by Poly-G Oligonucleotides of Different Lengths. Imino proton NMR spectra of DNA sequences d(TTG$_n$T) (termed ***Gn***) containing n continuous guanines (n = 12−19, Table 1) are shown in Figure 1. For

Table 1. DNA Sequences Analyzed in This Study

name	sequence (5′−3′)
G12	TTGGGGGGGGGGGT
G13	TTGGGGGGGGGGGGT
G14	TTGGGGGGGGGGGGGT
G15	TTGGGGGGGGGGGGGGT
T95-2T	TTGGGTGGGTGGGTGGGT
C95-2T	TTGGGCGGGCGGGCGGGT
A95-2T	TTGGGAGGGAGGGAGGGT
S95-2T[a]	TTGGGSGGGSGGGSGGGT
G16	TTGGGGGGGGGGGGGGGT
G17	TTGGGGGGGGGGGGGGGGT
G18	TTGGGGGGGGGGGGGGGGGT
G19	TTGGGGGGGGGGGGGGGGGGT

[a]S represents a dSpacer.

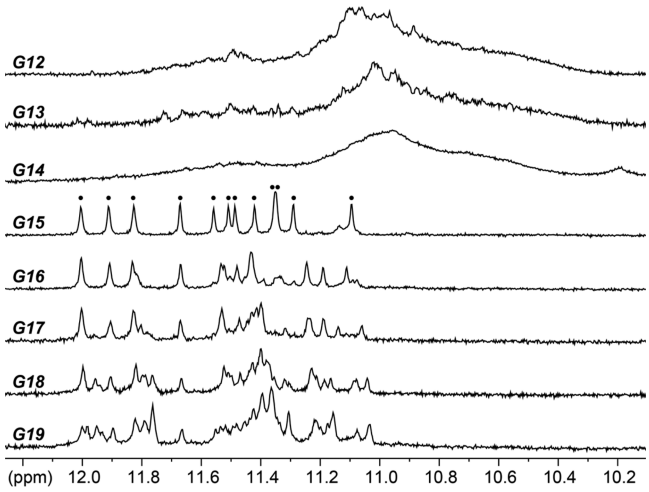

Figure 1. Imino proton spectra of the ***Gn*** sequences in solution containing 10 mM Tris (pH 7) and 2 mM KCl at 25 °C. Name of the sequences are labeled on top of each spectrum.

dx.doi.org/10.1021/bi500990v | *Biochemistry* 2014, 53, 7718−7723

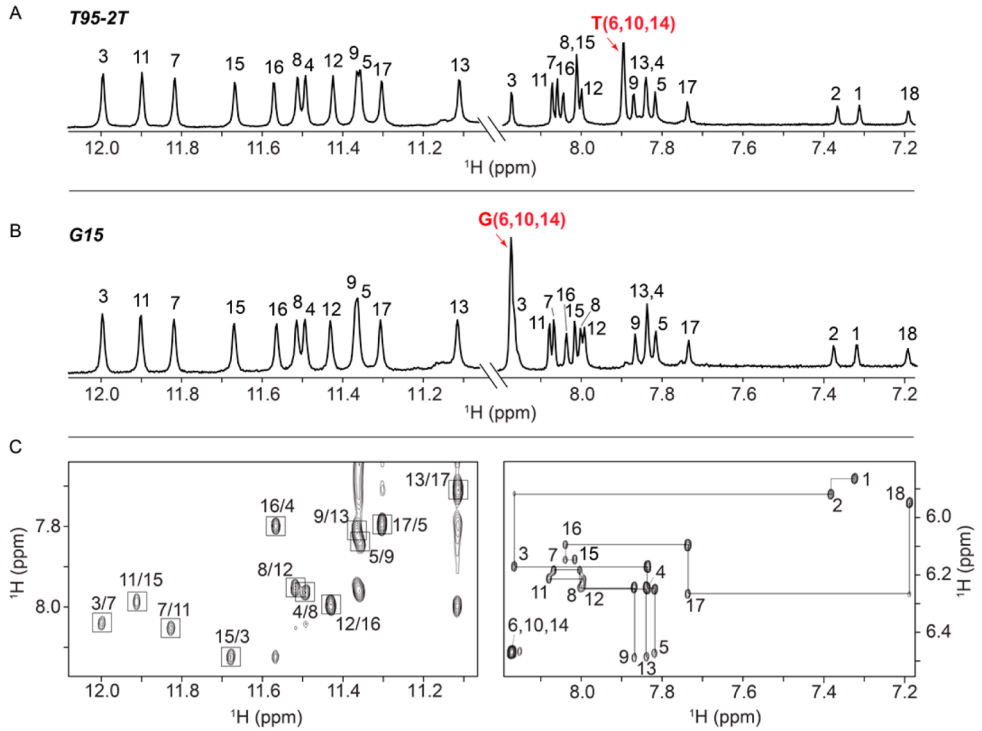

Figure 2. Proton NMR spectra of ***T95-2T*** and ***G15*** in solution containing 10 mM Tris (pH 7) and 2 mM KCl at 25 °C. (A and B) Imino and aromatic proton spectra of (A) ***T95-2T*** and (B) ***G15***. NMR spectra of the two sequences are almost identical, except for the aromatic protons of the loop residues 6, 10, and 14 (labeled in red). (C) NOESY spectra of ***G15*** (mixing time, 300 ms): (Left) Imino-H8 proton region showing characteristic guanine imino-H8 cross-peaks for G-tetrads, which are framed and labeled with the assignment of the imino proton in the first position and that of the H8 proton in the second position. (Right) H8/H6−H1′ proton region showing NOE sequential connectivities. Intraresidue cross-peaks are labeled with the corresponding residue numbers. Moderate intensities of the cross-peaks between H8 and H1′ protons indicate *anti* glycosidic conformations of all guanines.

n < 15, imino proton spectra show a broad hump, suggesting the formation of high-order structures and/or a mixture of multiple conformations. Remarkably, for n = 15 the ***G15*** sequence displays an extremely well-resolved spectrum with distinct imino proton peaks in the 10−12 ppm range, characteristic of the formation of a well-defined G-quadruplex conformation. For n > 15, more peaks appeared in addition to the set of peaks observed in ***G15***, suggesting that a similar G-quadruplex as ***G15*** coexist with additional G-quadruplex conformation(s). The number of peaks increased as n increased with several peaks also merging together and giving rise to broadened peaks, consistent with the formation of multiple conformations. The CD spectra of all ***Gn*** sequences studied show a maximum around 260 nm and a minimum around 240 nm (Figure S1 of the Supporting Information), characteristic of parallel-stranded G-quadruplexes.[50]

NMR Structure of a G_{15} Stretch. We set out to determine the solution structure of the G-quadruplex formed by the ***G15*** sequence containing 15 continuous guanines, which showed an exceptionally well-resolved NMR spectrum. The monomeric nature of ***G15*** was indicated in a gel electrophoresis experiment (Figure S2 of the Supporting Information). The imino proton spectrum of ***G15***, which displays 12 sharp peaks, is almost identical to that of the reference sequence ***T95-2T*** studied previously;[46] the aromatic proton spectrum of ***G15*** is also very similar to that of ***T95-2T*** except for the positions of peaks of residues 6, 10, and 14 (G6, G10, and G14 in ***G15*** vs T6, T10, and T14 in ***T95-2T***, respectively) (Figure 2). The ***T95-2T*** sequence[46] was previously shown to adopt a propeller-type parallel-stranded three-layered G-quadruplex with three single-residue propeller (or double-chain-reversal) loops T6, T10, and T14 (Figure S3 of the Supporting Information). The striking similarity between the 1D and 2D NMR spectra of ***G15*** and those of ***T95-2T*** (Figure 2 and data not shown) indicates that ***G15*** adopts the same fold as that of ***T95-2T***, i.e. a propeller-type parallel-stranded G-quadruplex involving three G-tetrad layers, where three guanines G6, G10, and G14, form three single-residue propeller loops (Figure S3 of the Supporting Information). All guanines adopt an *anti* glycosidic conformation. This fold was confirmed by the NOESY spectra of ***G15*** (Figure 2).

The structure of ***G15*** (Figure 3) was determined on the basis of NMR restraints (Table 2). This structure is a three-layer propeller-type parallel-stranded G-quadruplex with three single-residue propeller loops. The first two thymines T1 and T2 are positioned on top of the upper G-tetrad with T2 being well

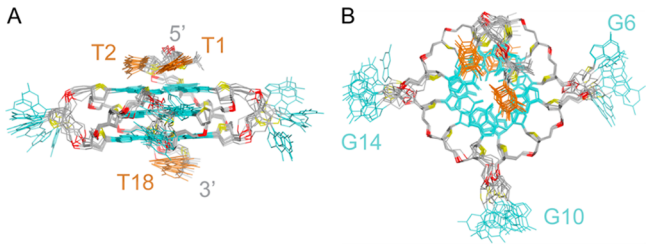

Figure 3. Solution structure of ***G15*** determined by NMR. (A) Side view and (B) top view of 10 superimposed lowest-energy structures. The bases of thymines are colored orange; guanines, cyan; backbone and sugar, gray; O4′ atoms, yellow; phosphorus atoms, red.

dx.doi.org/10.1021/bi500990v | *Biochemistry* 2014, 53, 7718−7723

Table 2. Statistics of the Computed Structures of the *G15* G-Quadruplex[a]

	D_2O	H_2O
A. NMR restraints		
distance restraints		
intraresidue	155	0
sequential (i, i+1)	91	11
long-range (i, ≥ i+2)	5	43
other restraints		
hydrogen bond	48	
dihedral angle	12	
repulsive	16	
B. Structure statistics		
NOE violations		
number (> 0.2 Å)	0.1 ± 0.0	
maximum violation (Å)	0.158 ± 0.025	
r.m.s.d. of violations (Å)	0.018 ± 0.002	
deviations from the ideal covalent geometry		
bond lengths (Å)	0.002 ± 0.000	
bond angles (deg)	0.665 ± 0.004	
impropers (deg)	0.328 ± 0.004	
pairwise all heavy atom r.m.s.d. values (Å)		
all heavy atoms except G6, G10, G14	0.73 ± 0.13	
all heavy atoms	1.77 ± 0.39	

[a]PDB ID 2MB2.

stacked on the G-tetrad and T1 slightly tilted. The thymine at the 3′ end (T18) is also stacked at the bottom G-tetrad. Indeed, the structure of ***G15*** is very similar to that of ***T95-2T*** (pairwise r.m.s.d. < 1 Å for all heavy atoms, excluding residues in the propeller loops), except that single-residue thymine loops are replaced by single-residue guanine loops (Figure 4).

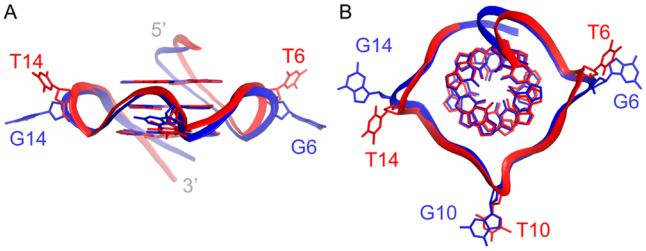

Figure 4. Comparison between the structures of ***G15*** (blue) and ***T95-2T*** (red). (A) Side view and (B) top view of a representative structure.

Single-Residue Propeller Loops. We hypothesized that any nucleotide (G, T, C, A, or even an abasic residue) could form a single-residue propeller loop bridging three G-tetrad layers of a parallel-stranded G-quadruplex. The loop residues G6, G10, G14 of ***G15*** were substituted by T, C, A, or S (a dSpacer−deoxyribose with no base) (Table 1). The imino proton NMR spectra of these sequences were almost identical to that of ***G15*** (Figure S4 of the Supporting Information), confirming that these sequences adopt the same propeller-type G-quadruplex fold. This conclusion was supported by the CD spectra of these sequences showing a positive peak at 260 nm, characteristic of a parallel G-quadruplex (Figure S5 of the Supporting Information).

The effect of loop residue on the stability of this propeller-type G-quadruplex was investigated using UV melting experiments (Figure S6 of the Supporting Information). The UV-melting data (Table 3) showed the highest melting temperature (T_m) for the sequence with loops containing no bases (dSpacer), very similar T_m values for sequences with thymine or cytosine loops, and a lower T_m value for the sequence with guanine loops, followed by that with adenine loops. This behavior can be attributed to the size differences between purines and pyrimidines and the ability of these bases to be hydrated or involved in secondary interactions. Our results agree well with the results previously reported for G-quadruplexes containing single-residue loops.[51,52]

Table 3. Thermodynamic Parameters for Propeller-Type G-Quadruplexes Containing Different Single-Residue Loops[a]

sequence name	T_m (°C)	ΔH (kcal/mol)	ΔS (kcal/mol/K)	ΔG (37 °C) (kcal/mol)
A95-2T	60.3	52.0	0.156	3.6
G15	66.0	58.4	0.172	4.9
C95-2T	75.6	79.1	0.227	8.7
T95-2T	75.6	86.8	0.249	9.5
S95-2T	>79.5	94.5	0.268	11.4

[a]All parameters listed were obtained using the transition direction from the G-quadruplex to single-strand (unfolding event).

Formation of *G15* Quadruplex Structure in a Long Poly-G Sequence. In principle, a poly-G sequence can form multiple G-quadruplexes involving different numbers of G-tetrads or different number residues in the loops, including possibilities of dynamic swapping between guanines in the G-tetrad core and loops.[42] The propeller-type G-quadruplex involving three G-tetrad layers and three single-residue propeller loops, which is formed by a sequence containing 15 continuous guanines, represents a unique well-defined robust scaffold that was observed as a single major conformation. Due to the repetitive nature of the sequence, the same G-quadruplex can be formed by a fragment of 15 continuous guanines anywhere along a poly-G sequence. Coincidently, among the poly-G tracts (G_n sequences) present in the genome of DOG-1-deficient *C. elegans*, DNA deletions were found exclusively for those with n > 14.[53] Thus, the unique ***G15*** quadruplex motif can be biologically relevant, being specifically recognized by proteins or other cellular molecules.

■ ASSOCIATED CONTENT

Ⓢ Supporting Information

Figures S1−S6 show additional experimental data (gel electrophoresis, CD spectra, NMR spectra, and UV melting curves). This material is available free of charge via the Internet at http://pubs.acs.org.

■ AUTHOR INFORMATION

Corresponding Author

*E-mail: phantuan@ntu.edu.sg. Phone: (+65) 6514 1915.

Funding

This research was supported by Singapore Ministry of Education Academic Research Fund Tier 3 (MOE2012-T3-1-001) and Tier 2 (MOE2012-T2-1-102), and grants from Nanyang Technological University to A.T.P.

Notes

The authors declare no competing financial interest.

■ REFERENCES

(1) Gellert, M., Lipsett, M. N., and Davies, D. R. (1962) Helix formation by guanylic acid. *Proc. Natl. Acad. Sci. U.S.A. 48*, 2013−2018.

(2) Sen, D., and Gilbert, W. (1988) Formation of parallel four-stranded complexes by guanine-rich motifs in DNA and its implications for meiosis. *Nature 334*, 364−366.
(3) Davis, J. T. (2004) G-quartets 40 years later: from 5′-GMP to molecular biology and supramolecular chemistry. *Angew. Chem., Int. Ed. 43*, 668−698.
(4) *Quadruplex Nucleic Acids*, Edited by Neidle, S. and Balasubramanian, S., 2006, Royal Society of Chemistry.
(5) Huppert, J. L., and Balasubramanian, S. (2005) Prevalence of quadruplexes in the human genome. *Nucleic Acids Res. 33*, 2908−2916.
(6) Todd, A. K., Johnston, M., and Neidle, S. (2005) Highly prevalent putative quadruplex sequence motifs in human DNA. *Nucleic Acids Res. 33*, 2901−2907.
(7) Rawal, P., Kummarasetti, V. B. R., Ravindran, J., Kumar, N., Halder, K., Sharma, R., Mukerji, M., Das, S. K., and Chowdhury, S. (2006) Genome-wide prediction of G4 DNA as regulatory motifs: role in *Escherichia coli* global regulation. *Genome Res. 16*, 644−655.
(8) Hershman, S. G., Chen, Q., Lee, J. Y., Kozak, M. L., Yue, P., Wang, L.-S., and Johnson, F. B. (2008) Genomic distribution and functional analyses of potential G-quadruplex-forming sequences in *Saccharomyces cerevisiae*. *Nucleic Acids Res. 36*, 144−156.
(9) Moyzis, R. K., Buckingham, J. M., Cram, L. S., Dani, M., Deaven, L. L., Jones, M. D., Meyne, J., Ratliff, R. L., and Wu, J. R. (1988) A highly conserved repetitive DNA sequence, $(TTAGGG)_n$, present at the telomeres of human chromosomes. *Proc. Natl. Acad. Sci. U.S.A. 85*, 6622−6626.
(10) Siddiqui-Jain, A., Grand, C. L., Bearss, D. J., and Hurley, L. H. (2002) Direct evidence for a G-quadruplex in a promoter region and its targeting with a small molecule to repress c-MYC transcription. *Proc. Natl. Acad. Sci. U.S.A. 99*, 11593−11598.
(11) Duquette, M. L., Handa, P., Vincent, J. A., Taylor, A. F., and Maizels, N. (2004) Intracellular transcription of G-rich DNAs induces formation of G-loops, novel structures containing G4 DNA. *Genes Dev. 18*, 1618−1629.
(12) Ribeyre, C., Lopes, J., Boulé, J. B., Piazza, A., Guédin, A., Zakian, V. A., and Mergny, J. L. (2009) The yeast Pif1 helicase prevents genomic instability caused by G-quadruplex-forming CEB1 sequences *in vivo*. *PLoS Genet. 5*, e1000475.
(13) Biffi, G., Tannahill, D., McCafferty, J., and Balasubramanian, S. (2013) Quantitative visualization of DNA G-quadruplex structures in human cells. *Nat. Chem. 5*, 182−186.
(14) Maizels, N., and Gray, L. T. (2013) The G4 genome. *PLoS Genet. 9*, e1003468.
(15) Lipps, H. J., and Rhodes, D. (2009) G-quadruplex structures: *in vivo* evidence and function. *Trends Cell Biol. 19*, 414−422.
(16) Balasubramanian, S., Hurley, L. H., and Neidle, S. (2011) Targeting G-quadruplexes in gene promoters: a novel anticancer strategy? *Nat. Rev. Drug Discov. 10*, 261−275.
(17) Patel, D. J., Phan, A. T., and Kuryavyi, V. (2007) Human telomere, oncogenic promoter and 5′-UTR G-quadruplexes: diverse higher order DNA and RNA targets for cancer therapeutics. *Nucleic Acids Res. 35*, 7429−7455.
(18) Cheung, I., Schertzer, M., Rose, A., and Lansdorp, P. M. (2002) Disruption of *dog-1* in *Caenorhabditis elegans* triggers deletions upstream of guanine-rich DNA. *Nat. Genet. 31*, 405−409.
(19) Zhao, Y., O'Neil, N. J., and Rose, A. M. (2007) Poly-G/poly-C tracts in the genomes of *Caenorhabditis*. *BMC Genomics 8*, 403.
(20) Snyder, L. A., Loman, N. J., Linton, J. D., Langdon, R. R., Weinstock, G. M., Wren, B. W., and Pallen, M. J. (2010) Simple sequence repeats in *Helicobacter canadensis* and their role in phase variable expression and C-terminal sequence switching. *BMC Genomics 11*, 67.
(21) Pernitzsch, S. R., Tirier, S. M., Beier, D., and Sharma, C. M. (2014) A variable homopolymeric G-repeat defines small RNA-mediated posttranscriptional regulation of a chemotaxis receptor in *Helicobacter pylori*. *Proc. Natl. Acad. Sci. U.S.A. 111*, E501−E510.
(22) Huppert, J. (2008) Hunting G-quadruplexes. *Biochimie 90*, 1140−1148.
(23) Collie, G. W., and Parkinson, G. N. (2011) The application of DNA and RNA G-quadruplexes to therapeutic medicines. *Chem. Soc. Rev. 40*, 5867−5892.
(24) Li, Z., and Mirkin, C. A. (2005) G-quartet-induced nanoparticle assembly. *J. Am. Chem. Soc. 127*, 11568−11569.
(25) Mukundan, V. T., Quang, M. N. T., Miao, Y., and Phan, A. T. (2013) Connecting magnetic micro-particles with DNA G-quadruplexes. *Soft Matter 9*, 216−223.
(26) Huang, Y. C., and Sen, D. (2010) A contractile electronic switch made of DNA. *J. Am. Chem. Soc. 132*, 2663−2671.
(27) Cai, J., Shapiro, E. M., and Hamilton, A. D. (2009) Self-assembling DNA quadruplex conjugated to MRI contrast agents. *Bioconjugate Chem. 20*, 205−208.
(28) Wang, K., You, M., Chen, Y., Han, D., Zhu, Z., Huang, J., Williams, K., Yang, C. J., and Tan, W. (2011) Self-assembly of a bifunctional DNA carrier for drug delivery. *Angew. Chem., Int. Ed. 50*, 6098−6101.
(29) Cavalieri, F., Ng, S. L., Mazzuca, C., Jia, Z., Bulmus, V., Davis, T. P., and Caruso, F. (2011) Thin multilayer films and microcapsules containing DNA quadruplex motifs. *Small 7*, 101−111.
(30) Chiorcea-Paquim, A. M., Santos, P. V., Eritja, R., and Oliveira-Brett, A. M. (2013) Self-assembled G-quadruplex nanostructures: AFM and voltammetric characterization. *Phys. Chem. Chem. Phys. 15*, 9117−9124.
(31) Kotlyar, A. B., Borovok, N., Molotsky, T., Cohen, H., Shapir, E., and Porath, D. (2005) Long, monomolecular guanine-based nanowires. *Adv. Mater. 17*, 1901−1905.
(32) Batalia, M. A., Protozanova, E., Macgregor, R. B., and Erie, D. A. (2002) Self-assembly of frayed wires and frayed-wire networks: nanoconstruction with multistranded DNA. *Nano Lett. 2*, 269−274.
(33) Burge, S., Parkinson, G. N., Hazel, P., Todd, A. K., and Neidle, S. (2006) Quadruplex DNA: sequence, topology and structure. *Nucleic Acids Res. 34*, 5402−5415.
(34) Phan, A. T., Kuryavyi, V., Burge, S., Neidle, S., and Patel, D. J. (2007) Structure of an unprecedented G-quadruplex scaffold in the human *c-kit* promoter. *J. Am. Chem. Soc. 129*, 4386−4392.
(35) Amrane, S., Adrian, M., Heddi, B., Serero, A., Nicolas, A., Mergny, J. L., and Phan, A. T. (2012) Formation of pearl-necklace monomorphic G-quadruplexes in the human CEB25 minisatellite. *J. Am. Chem. Soc. 134*, 5807−5816.
(36) Marusic, M., Sket, P., Bauer, L., Viglasky, V., and Plavec, J. (2012) Solution-state structure of an intramolecular G-quadruplex with propeller, diagonal and edgewise loops. *Nucleic Acids Res. 40*, 6946−6956.
(37) Mukundan, V. T., and Phan, A. T. (2013) Bulges in G-quadruplexes: broadening the definition of G-quadruplex-forming sequences. *J. Am. Chem. Soc. 135*, 5017−5028.
(38) Wei, D., Todd, A. K., Zloh, M., Gunaratnam, M., Parkinson, G. N., and Neidle, S. (2013) Crystal structure of a promoter sequence in the *B-raf* gene reveals an intertwined dimer quadruplex. *J. Am. Chem. Soc. 135*, 19319−19329.
(39) Lim, K. W., and Phan, A. T. (2013) Structural basis of DNA quadruplex-duplex junction formation. *Angew. Chem., Int. Ed. 52*, 8566−8569.
(40) Chen, Y., Agrawal, P., Brown, R. V., Hatzakis, E., Hurley, L., and Yang, D. (2012) The major G-quadruplex formed in the human platelet-derived growth factor receptor beta promoter adopts a novel broken-strand structure in K^+ solution. *J. Am. Chem. Soc. 134*, 13220−13223.
(41) Karsisiotis, A. I., O'Kane, C., and Webba da Silva, M. (2013) DNA quadruplex folding formalism − A tutorial on quadruplex topologies. *Methods 64*, 28−35.
(42) Adrian, M., Ang, D. J., Lech, C. J., Heddi, B., Nicolas, A., and Phan, A. T. (2014) Structure and conformational dynamics of a stacked dimeric G-quadruplex formed by the human CEB1 minisatellite. *J. Am. Chem. Soc. 136*, 6297−6305.
(43) Phillips, K., Dauter, Z., Murchie, A. I., Lilley, D. M., and Luisi, B. (1997) The crystal structure of a parallel-stranded guanine tetraplex at 0.95 Å resolution. *J. Mol. Biol. 273*, 171−182.

(44) Joly, L., Rosu, F., and Gabelica, V. (2012) d(TG_nT) DNA sequences do not necessarily form tetramolecular G-quadruplexes. *Chem. Commun. 48*, 8386−8388.
(45) Panyutin, I. G., Kovalsky, O. I., Budowsky, E. I., Dickerson, R. E., Rikhirev, M. E., and Lipanov, A. A. (1990) G-DNA: a twice-folded DNA structure adopted by single-stranded oligo(dG) and its implications for telomeres. *Proc. Natl. Acad. Sci. U.S.A. 87*, 867−870.
(46) Do, N. Q., and Phan, A. T. (2012) Monomer-dimer equilibrium for the 5′-5′ stacking of propeller-type parallel-stranded G-quadruplexes: NMR structural study. *Chem. Eur. J. 18*, 14752−14759.
(47) Phan, A. T., Guéron, M., and Leroy, J. L. (2002) Investigation of unusual DNA motifs. *Meth. Enzymol. 338*, 341−371.
(48) Schwieters, C. D., Kuszewski, J. J., Tjandra, N., and Marius Clore, G. (2003) The Xplor-NIH NMR molecular structure determination package. *J. Magn. Reson. 160*, 65−73.
(49) DeLano, W. L., and Bromberg, S. (2004) *PyMOL user's guide*, DeLano Scientific LLC.
(50) Gray, D. M., Wen, J. D., Gray, C. W., Repges, R., Repges, C., Raabe, G., and Fleischhauer, J. (2008) Measured and calculated CD spectra of G-quartets stacked with the same or opposite polarities. *Chirality 20*, 431−440.
(51) Rachwal, P. A., Brown, T., and Fox, K. R. (2007) Sequence effects of single base loops in intramolecular quadruplex DNA. *FEBS Lett. 581*, 1657−1660.
(52) Guédin, A., De Cian, A., Gros, J., Lacroix, L., and Mergny, J. L. (2008) Sequence effects in single-base loops for quadruplexes. *Biochimie 90*, 686−696.
(53) Kruisselbrink, E., Guryev, V., Brouwer, K., Pontier, D. B., Cuppen, E., and Tijsterman, M. (2008) Mutagenic capacity of endogenous G4 DNA underlies genome instability in FANCJ-defective *C. elegans*. *Curr. Biol. 18*, 900−905.